Exploration of the basic reactant in CO_2 photoreduction: New insights from photophysics and photochemistry

Duanhui Si, Xuedan Song*, Heming Zhang, Yantao Shi, Ce Hao

State Key Laboratory of Fine Chemicals, School of Chemistry, Dalian University of Technology, Dalian, 116024, Liaoning, China

ABSTRACT

Photoreduction of CO_2 as an attractive path for CO_2 conversion has drawn widespread interest. Experiments demonstrating the photoreduction of CO_2 are conducted in water solution in the excited state, and solvent molecules play a major role in the reaction mechanism. Thus, a simple gas-phase CO_2 model of the ground-state cannot fully demonstrate the characteristics of aqueous CO_2 and the mechanisms of CO_2 photoreduction in the excited state. A deep understanding of the characteristics of aqueous CO_2 as the basic reactant is the cornerstone for the development of photocatalysts. In this study, a systemic investigation involving photophysics and photochemistry was performed to determine its existential status, kinetic and thermodynamic characteristics. In the excited state, H_2CO_3 as the main inorganic carbon in pure water should be considered in the photoreduction of CO_2, and the development of photocatalysts should compatible with its characteristics.

1. Introduction

Photoreduction of carbon dioxide (CO_2) is considered an excellent method that can potentially solve global warming and energy shortage worldwide [1–4]. During photoreduction, CO_2 is activated under light radiation and converted in the excited state [5]. Experiments in the photoreduction of CO_2 are usually conducted in a water solution [1–4,6,7]. Their mechanisms are explored using the gas-phase CO_2 model in the ground state as the base substrate [8–11]. However, the characteristics of CO_2 in a water solution and the gas phase are varied [12,13]. The substrate characteristics in the ground state and the excited state are also differ to a greater extent [14,15]. Consequently, merely using the simple gas-phase CO_2 model of the ground state to study the mechanisms of CO_2 photoreduction requires more improvement. To address this concern, the characteristics of CO_2 in water solution (namely aqueous CO_2) in the excited state should be investigated, and suitable photocatalysts compatible with its characteristics should be developed.

The mechanisms underlying the photoreduction of CO_2 involve complex photophysical transition and photochemical reaction. Investigation of photophysics and photochemistry provides valuable information. For instance, competition of photophysical transitions and the lifetime of excited states can determine the fate of the CO_2 molecules in the excited state [16,17]. The activation energy (E_a), Gibbs free energy of activation ($\Delta_r G$) and the relative energy of each stationary point reveal the of kinetic and thermodynamic characteristics [18,19]. Thus, the photophysics and photochemistry characteristics of aqueous CO_2 as the basic reactant are of great importance to obtain an in-depth understanding of CO_2 photoreduction.

In this study, the aqueous CO_2 in the excited state was explored from the photophysical and photochemical perspectives by using Time-dependent density functional theory (TDDFT). TDDFT plays a key role in the study of excited state [20,21]. Activation of aqueous CO_2 was discussed by the geometry change and charge transfer. The rate constants of the photophysical and photochemical processes further explored its existential status in the excited state.

2. Calculation method

2.1. Theory

Photophysics includes radiative transition (fluorescence emission and phosphorescence emission) and non-radiative transition (internal conversion and intersystem crossing). In aqueous CO_2, the rate constants of radiative transition are considerably lower than that of non-radiative transition, which is listed in Table S1. Thus, the radiative transition is neglected. Here, the photophysics involves three processes: (i) internal conversion (IC) of aqueous CO_2 transferred from the first excited singlet state (S_1) to the ground state (S_0); (ii) intersystem crossing (ISC) of aqueous CO_2 transferred from the S_1 state to the first
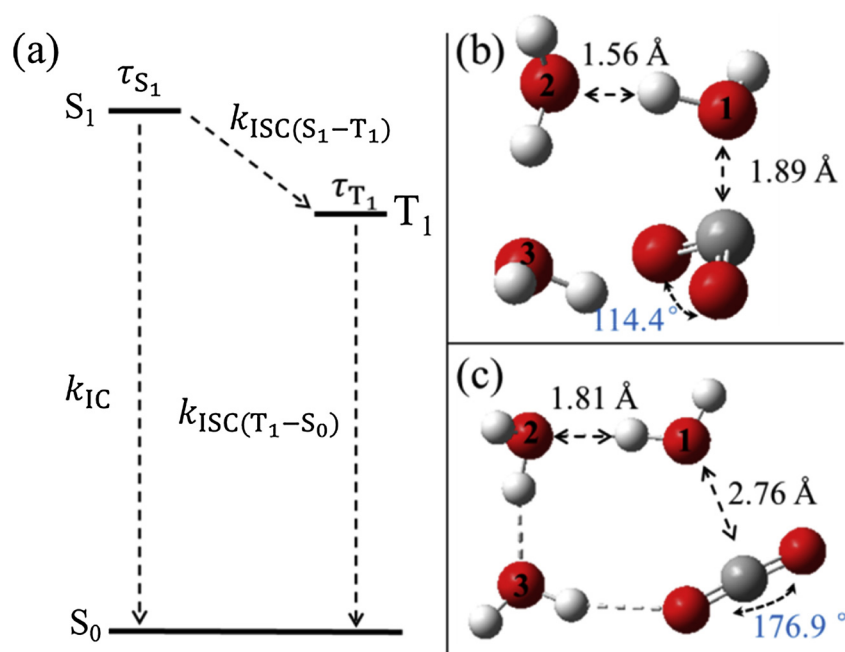

Fig. 1. Photophysics of aqueous CO_2 (a), the structures of aqueous CO_2 in the S_1 state (b) and the S_0 state (c). k means the rate constant, τ indicates the lifetime. The water molecules are labeled as 1-H_2O, 2-H_2O and 3-H_2O, respectively, which are presented on the oxygen atom. Text in black denotes the bond length and text in blue denotes the bond angle. The grey ball, white ball and red ball indicate the C, H, and O atoms, respectively.

excited triplet state (T_1); (iii) the ISC of aqueous CO_2 transferred from the T_1 state to the S_0 state. The rate constants of IC and ISC are calculated as follows: [16,17]

$$k_{IC} = \frac{2\pi}{h} \sum_{u,v} P_{iv}(T) \left| \sum_{n} \langle \Phi_f | \hat{P}_n | \Phi_i \rangle \langle \Theta_{fu} | \hat{P}_n | \Theta_{iv} \rangle \right|^2 \delta(E_{iv} - E_{fu})$$

$$k_{ISC} = \frac{2\pi}{h} \sum_{u,v} P_{iv}(T) |\langle \Phi_f | \hat{H}^{SO} | \Phi_i \rangle|^2 |\langle \Theta_{fu} | \Theta_{iv} \rangle|^2 \delta(E_{iv} - E_{fu})$$

where k is the rate constant; h is the Planck constant; P_{iv} is the Boltzmann distribution of the initial state; T is the temperature; Φ represents the electronic state; Θ is the vibrational wavefunction; $\hat{P}_n$ indicates the momentum operator of the nth normal vibrational mode in the final state; $\hat{H}^{SO}$ denotes the Hamiltonian operator of spin-orbit coupling; E indicates the energy; i and f are the initial and the final state, respectively; v and u are the vibrational quantum numbers of the initial state and the final state, respectively.

The reaction rate constant is obtained from Arrhenius equation [22–25].

$$k_r = \left(1 + \frac{1}{24} \times \left(\frac{\hbar v_i}{k_b \times T}\right)^2\right) \times \frac{k_b \times T}{h} \times e^{-\frac{\Delta_r G}{RT}}$$

where k_b is the Boltzmann constant and $\Delta_r G$ is the Gibbs free energy of activation, which is calculated by comparing the Gibbs free energies between the transition state and the reactant; R is the gas constant; v_i is the imaginary frequency of the transition state, which is listed in Table S5.

The amount of charge transfer of fragment A during electron excitation is calculated as follows:

$$Q_A = q_{A,ex} - q_{A,gs}$$

where Q is the amount of charge transfer; q is the charge of the fragment, which is derived by summing up the atom charge of the fragment; gs and ex are the ground state and the excited state, respectively.

2.2. Calculation details

The integral equation formalism of polarized continuum model (IEFPCM) [26] as the solvent model, in conjunction with the B3LYP hybrid functional [27], was adopted in all calculations by using the Gaussian 16 program [28]; the ground state (S_0) and excited state (S_1 and T_1) were calculated by density functional theory (DFT) and TDDFT, respectively [29,30]. Geometry optimization, vibrational frequency calculation, activation energy (E_a), Gibbs free energy of activation ($\Delta_r G$), Gibbs free energy of change (ΔG), and the atomic dipole corrected Hirshfeld (ADCH) atomic charge [31] were performed at the level of 6-311G + + (d,p) basis set [32,33]. These results were analyzed by using Multiwfn software [34]. The dispersion correction was considered using D3BJ [35,36], and the temperature was set to 298 K in calculating Gibbs free energy and photophysics. The photophysics was calculated using the MOMAP software [16,17,37,38].

3. Results and discussion

As reported in previous quantum studies of CO_2 reaction with H_2O in the ground state, the solvent water molecules evidently affected E_a [12,13]. To adequately evaluate the effect of water molecules, the different number (from one to four) of water molecules that participated in the reaction was calculated. As shown in Figure S1, the E_a (17.2 kcal mol^{-1}) of H_2CO_3 formed from one carbon dioxide molecule and three water molecules was consistent with the experimental value (17.7 kcal mol^{-1}) [39]. Moreover, CO_2 as the main inorganic carbon exists in pure water in the ground state [40]. Thus, we adopted one carbon dioxide molecule and three water molecules as the primitive model to reveal the characteristics of aqueous CO_2 in the excited state.

3.1. Photophysics of aqueous CO_2

As shown in Fig. 1a, the photophysics of aqueous CO_2 has three non-radiative transition paths: IC, ISC($S_1 - T_1$) and ISC($T_1 - S_0$). The rate constants k_{IC} and $k_{ISC(S_1-T_1)}$ are 2.2×10^3 s^{-1} and 3.6×10^7 s^{-1}, respectively (see Table 1). Thus, aqueous CO_2 in the S_1 state prefers to shift to the T_1 state, and only a fraction of them return to the S_0 state.

Table 1
The theoretical parameters in the photophysics and photochemistry.

Photophysics	Parameters		CO_2	H_2CO_3
	The rate constant (s^{-1})	k_{IC}	2.2×10^3	2.1×10^{10}
		$k_{ISC(S_1-T_1)}$	3.6×10^7	5.3×10^6
		$k_{ISC(T_1-S_0)}$	5.0×10^8	1.9×10^7
	The lifetime (s)	τ_{S_1}	1.7×10^{-8}	4.8×10^{-11}
		τ_{T_1}	2.0×10^{-9}	5.3×10^{-8}
Photochemistry	Rate constants (s^{-1})		Forward	Reverse
	Reaction 1		6.2×10^{12}	2.0×10^7
	Reaction 2		1.2×10^{12}	1.5×10^{11}

After aqueous CO_2 reaches the T_1 state, it returns to the S_0 state, and the $k_{ISC(T_1-S_0)}$ is 5.0×10^8 s^{-1}. The lifetimes τ_{S_1} and τ_{T_1} are 1.7×10^{-8} s and 2.0×10^{-9} s, respectively. In this way, aqueous CO_2 in the excited state mainly existed in the S_1 state. We investigated the aqueous CO_2 in the excited state by comparing its characteristics in the S_0 and S_1 states.

There are three water molecules in this system, which labeled 1-H_2O, 2-H_2O and 3-H_2O. As shown in Figs. 1b and 1c, the structure of aqueous CO_2 evidently changed during excitation. The length between the C atom (CO_2) and the O atom (1-H_2O) changes from 2.76 Å to

1.89 Å, which is shortened by 0.87 Å. The intermolecular hydrogen bond between the H atom (1-H_2O) and the O atom (2-H_2O) changes from 1.81 Å to 1.56 Å, indicating that the intermolecular hydrogen bond becomes stronger. Moreover, the bond angle of CO_2 changes from 176.9° to 114.4°. Thus, the inert linear structure of the CO_2 transferred to the V-type structure, which affects the charge distribution and further activates the aqueous CO_2. More details about the structures of aqueous CO_2 are shown in Figure S2 and Table S1.

The ADCH charge as the correction of Hirshfeld charge provides accurate distribution of atomic charge and has very good electrostatic potential reproducibility. Thus, we used it to quantitatively investigate the charge transfer during excitation. As shown in Fig. 2, the ADCH charges of CO_2, 2-H_2O and 3-H_2O all become more negative from 0.021, 0.002 and 0.073 in the S_0 state to -0.561, -0.105 and 0.029 in the S_1 state. Only ADCH charges of 1-H_2O become more positive from -0.097 to 0.638. Thus, electron transfers from 1-H_2O to other molecules. In other words, the CO_2 and water molecules are activated. The distance between the O atom of 1-H_2O and the neighbouring the C atom of CO_2 decreases from 2.76 Å to 1.89 Å, which may play an important role during the activation. More details about ADCH charges were presented in Table S3.
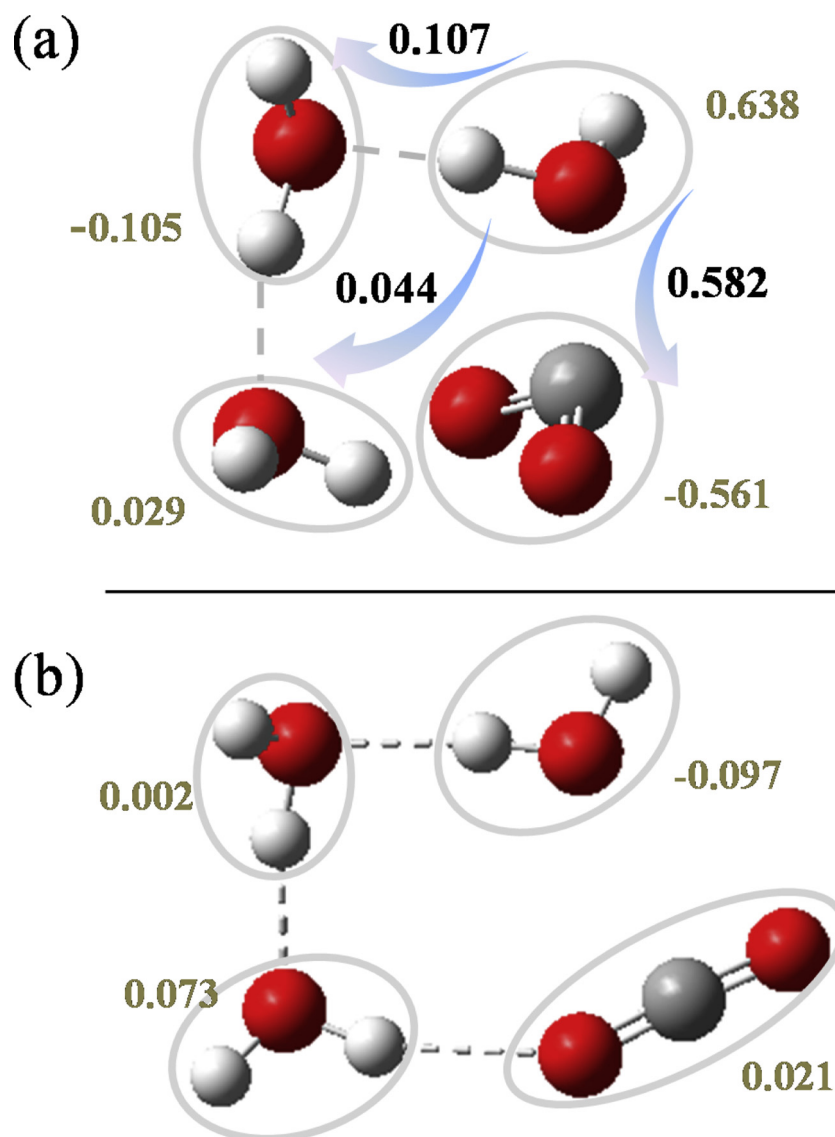

Fig. 2. The transfer of ADCH charge of aqueous CO_2 during excitation. The ADCH charge of aqueous CO_2 in the S_1 state (a) and the S_0 state (b). The tan text denotes ADCH charge of molecules and the black text denotes the amount of ADCH charge transfer.
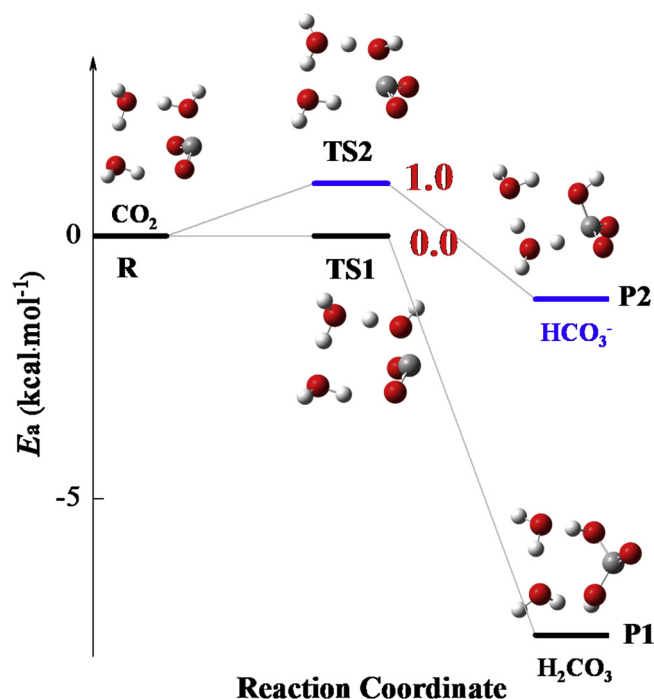
Fig. 3. Formation mechanisms of H_2CO_3 and HCO_3^- from CO_2 and 3 H_2O. The black line represents H_2CO_3 formation (Reaction 1) and blue line represents HCO_3^- formation (Reaction 2).

3.2. Photochemistry of aqueous CO_2

After the system is excited to the S_1 state, photochemical reactions can initiate. As shown in Fig. 3, CO_2 react with water molecules to generate H_2CO_3 and HCO_3^-. The corresponding E_a were 0.0 and 1.0 kcal mol^{-1}, respectively. The reaction selectivity was determined by the direction of the C=O bond of the CO_2 molecule. H_2CO_3 is formed (Reaction 1) when the C=O bond is facing to the 3-H_2O molecule; HCO_3^- is generated (Reaction 2) when the C=O bond deviates from the 3-H_2O molecule.

The rate constant of H_2CO_3 formation is 6.2×10^{12} s^{-1}, which is

five orders of magnitude larger than that of the reverse reaction (see Table 1). The rate constant of HCO_3^- formation was 1.2×10^{12} s^{-1}, which is one order of magnitude larger than that of the reverse reaction. Thus, from the kinetic perspective, H_2CO_3 is the dominant form of inorganic carbon in the excited state. HCO_3^- and CO_2 make up small proportion. In addition, the rate constant of aqueous CO_2 to generate H_2CO_3 is markedly significantly larger than $k_{ISC(S_1-T_1)}$ and k_{IC}, indicating that most of aqueous CO_2 in the S_1 state tend to generate H_2CO_3 instead of performing photophysical transitions to S_0 and T_1 states.

The thermodynamic process was investigated using ΔG, obtained by comparing the Gibbs free energies of the product and the reactant. The ΔG of H_2CO_3 and HCO_3^- formation are -7.2 and 0.0 kcal mol^{-1}, respectively, indicating that they were spontaneous reactions from the thermodynamic perspective. In particular, the ΔG of H_2CO_3 formation was smaller than that of HCO_3^- formation, demonstrating that H_2CO_3 was more stable than HCO_3^- and CO_2 in the excited state. Thus, in the excited state H_2CO_3 is the dominant form.

3.3. Photophysics of aqueous H_2CO_3

We further investigated the photophysical process of H_2CO_3 to investigate its fate in the excited state. As shown in Fig. 4a, there are three transition paths and the corresponding rate constants are listed in Table 1. The k'_{IC} and $k_{ISC(S_1-T_1)}$ are calculated to be 2.1×10^{10} s^{-1} and 5.3×10^6 s^{-1}, respectively. Thus, the aqueous H_2CO_3 in the S_1 state prefers to return to the S_0 state, and only a fraction can transfer to the T_1 state, which may be the reason for the low yield of CO_2 photoreduction in the triplet state. After aqueous H_2CO_3 reaches the T_1 state it also has a path to return to the S_0 state. The corresponding rate constant $k'_{ISC(T_1-S_0)}$ is 1.9×10^7 s^{-1}. The lifetimes τ'_{S_1} and τ'_{T_1} are calculated as 4.7×10^{-11} s and 5.3×10^{-8} s, respectively. Thus, after aqueous H_2CO_3 reaches T_1 state it has a longer lifetime than in the S_1 state. Furthermore, the τ'_{T_1} was much larger than τ_{S_1}, we proposed that aqueous H_2CO_3 as the major reaction substrate should be considered in the photoreduction of CO_2 in the triplet state.

The structure and ADCH charge of aqueous H_2CO_3 in the T_1 state were explored to reveal its characteristics. The structure of aqueous H_2CO_3 significantly changed from the T_1 state (Fig. 3b) to the S_0 state (Fig. 3c). The bond of C1-O2 changed from a single bond with a length of 1.50 Å to a double bond with a length of 1.21 Å. Thus, the bond energy of C1-O2 in the T_1 state is weaker and more easily fractured.
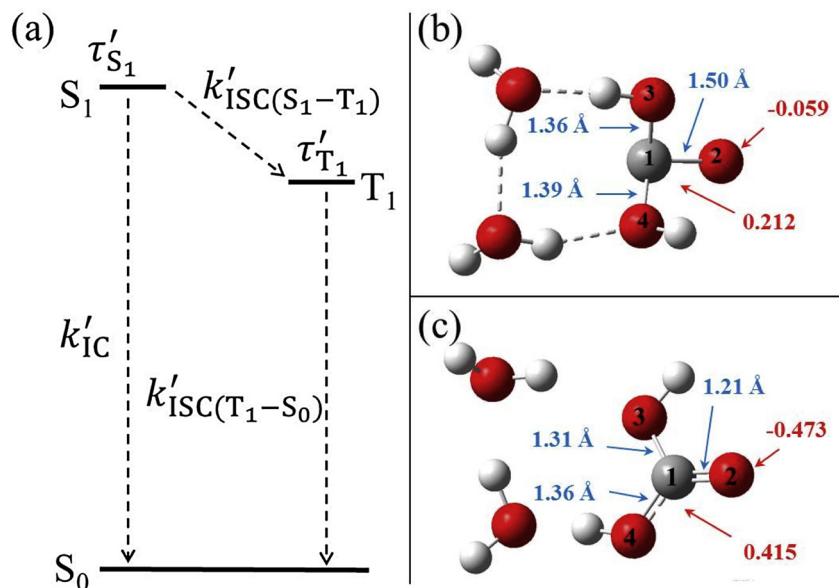

Fig. 4. Photophysics of aqueous H_2CO_3 (a), the structure of aqueous H_2CO_3 in the T_1 state (b) and the S_0 state (c). The black texts on the atoms denote atomic number, the red texts denote ADCH charge and the blue texts denote the bond length.

These results were confirmed by the change of ADCH charge. The ADCH charge of the O2 atom increases from -0.473 to -0.059, whereas that of the C1 atom decreases from 0.415 to 0.212. Thus, the O2 atom preferred to react with the neighbouring catalyst in the T_1 state. Considering all the characteristics of aqueous H_2CO_3 in the T_1 state, H_2CO_3 is the main form of substrate in the photoreduction of CO_2.

4. Conclusions

The characteristics of aqueous CO_2 in the excited state were systematically investigated by photophysics and photochemistry. By comparing a series of rate constants of photophysical process, we concluded that the aqueous CO_2 of the excited state existed in the S_1 state and aqueous H_2CO_3 of the excited state existed in the T_1 state. Moreover, from the kinetic and thermodynamic perspectives, inorganic carbon of the excited state constituted a large amount of H_2CO_3, with a fraction of HCO_3^- and CO_2 in pure water. Thus, aqueous H_2CO_3 as a major reaction substrate should be considered in the photoreduction of CO_2, and the development of photocatalysts should be suitable to its characteristics.

Declaration of Competing Interest

There are no conflicts to declare.

Acknowledgements

Appendix A. Supplementary data

Supplementary material related to this article can be found, in the online version, at doi:https://doi.org/10.1016/j.jphotochem.2019.111959.

References

[1] X. Liu, S. Inagaki, J. Gong, Heterogeneous molecular systems for photocatalytic CO_2 reduction with water oxidation, Angew. Chem. Int. Ed. 55 (2016) 14924–14950, https://doi.org/10.1002/anie.201600395.

[2] M. Marszewski, S. Cao, J. Yu, M. Jaroniec, Semiconductor-based photocatalytic CO_2 conversion, Mater. Horiz. 2 (2015) 261–278, https://doi.org/10.1039/c4mh00176a.

[3] Y. Ma, X. Wang, Y. Jia, X. Chen, H. Han, C. Li, Titanium dioxide-based nanomaterials for photocatalytic fuel generations, Chem. Rev. 114 (2014) 9987–10043, https://doi.org/10.1021/cr500008u.

[4] A.J. Morris, G.J. Meyer, E. Fujita, Molecular approaches to the photocatalytic reduction of carbon dioxide for solar fuels, Acc. Chem. Res. 42 (2009) 1983–1994, https://doi.org/10.1021/ar9001679.

[5] X. He, W.N. Wang, MOF-based ternary nanocomposites for better CO_2 photoreduction: roles of heterojunctions and coordinatively unsaturated metal sites, J. Mater. Chem. A Mater. Energy Sustain. 6 (2018) 932–940, https://doi.org/10.1039/C7TA09192C.

[6] J. Kou, C. Lu, J. Wang, Y. Chen, Z. Xu, R.S. Varma, Selectivity enhancement in heterogeneous photocatalytic transformations, Chem. Rev. 117 (2017) 1445–1514, https://doi.org/10.1021/acs.chemrev.6b00396.

[7] C. Peng, G. Reid, H. Wang, P. Hu, Perspective: photocatalytic reduction of CO_2 to solar fuels over semiconductors, J. Chem. Phys. 147 (2017) 030901, , https://doi.org/10.1063/1.4985624.

[8] V.P. Indrakanti, J.D. Kubicki, H.H. Schobert, Quantum chemical modeling of ground states of CO_2 chemisorbed on anatase (001),(101), and (010) TiO_2 surfaces, Energy Fuels 22 (2008) 2611–2618, https://doi.org/10.1021/ef700725u.

[9] S. Ma, W. Song, B. Liu, W. Zhong, J. Deng, H. Zheng, H. Zheng, J. Liu, X. Gong, Z. Zhao, Facet-dependent photocatalytic performance of TiO_2: a DFT study, Appl. Catal. B-Environ. 198 (2016) 1–8, https://doi.org/10.1016/j.apcatb.2016.05.017.

[10] L. Li, R. Zhang, J. Vinson, E.L. Shirley, J.P. Greeley, J.R. Guest, M.K.Y. Chan, Imaging catalytic activation of CO_2 on Cu_2O (110): a first-principles study, Chem. Mat. 30 (2018) 1912–1923, https://doi.org/10.1021/acs.chemmater.7b04803.

[11] B. Modak, P. Modak, S.K. Ghosh, Improving visible light photocatalytic activity of $NaNbO_3$: a DFT based investigation, RSC Adv. 6 (2016) 90188–90196, https://doi.org/10.1039/C6RA15024A.

[12] X. Wang, W. Conway, R. Burns, N. McCann, M. Maeder, Comprehensive study of the hydration and dehydration reactions of carbon dioxide in aqueous solution, J. Phys. Chem. A 114 (2009) 1734–1740, https://doi.org/10.1021/jp909019u.

[13] M.T. Nguyen, M.H. Matus, V.E. Jackson, V.T. Ngan, J.R. Rustad, D.A. Dixon, Mechanism of the hydration of carbon dioxide: direct participation of H_2O versus microsolvation, J. Phys. Chem. A 112 (2008) 10386–10398, https://doi.org/10.1021/jp804715j.

[14] G.J. Zhao, K.L. Han, Hydrogen bonding in the electronic excited state, Accounts Chem. Res. 45 (2011) 404–413, https://doi.org/10.1021/ar200135h.

[15] S.J. Formosinho, L.G. Arnaut, Excited-state proton transfer reactions II. Intramolecular reactions, J. Photochem. Photobiol. A Chem. 75 (1993) 21–48, https://doi.org/10.1016/1010-6030(93)80158-6.

[16] Y. Niu, Q. Peng, Z.G. Shuai, Promoting-mode free formalism for excited state radiationless decay process with Duschinsky rotation effect, Sci. China Ser. B Chem. Life Sci. Earth Sci. 51 (2008) 1153–1158, https://doi.org/10.1007/s11426-008-0130-4.

[17] Q. Peng, Y. Niu, Q. Shi, Correlation function formalism for triplet excited state decay: combined spin-orbit and nonadiabatic couplings, J. Chem. Theor. Comput. 9 (2013) 1132–1143, https://doi.org/10.1021/ct300798t.

[18] H. Zhang, X. Song, J. Liu, C. Hao, Photophysics and photochemical insights of the photodegradation of norfloxacin: the rate-limiting step and the influence of Ca^{2+} ion, Chemosphere 219 (2019) 236–242, https://doi.org/10.1016/j.chemosphere.2018.11.198.

[19] L. Shen, Theoretical study on the photophysics and photochemical properties of elsinochrome a, J. Biomol. Struct. Dyn. 25 (2007) 321–325, https://doi.org/10.1080/07391102.2007.10507180.

[20] P. Zhou, K. Han, Unraveling the detailed mechanism of excited-state proton transfer, Acc. Chem. Res. 51 (2018) 1681–1690, https://doi.org/10.1021/acs.accounts.8b00172.

[21] C. Adamo, D. Jacquemin, The calculations of excited-state properties with time-dependent density functional theory, Chem. Soc. Rev. 42 (2013) 845–856, https://doi.org/10.1039/c2cs35394f.

[22] H. Eyring, The activated complex in chemical reactions, J. Chem. Phys. 3 (1935) 107–115, https://doi.org/10.1063/1.1749604 107-115..

[23] E. Wigner, Calculation of the rate of elementary association reactions, J. Chem. Phys. 5 (1937) 720–725, https://doi.org/10.1063/1.1750107.

[24] E. Wigner, Über das Überschreiten von Potentialschwellen bei chemischen Reaktionen, Zeitschrift für Physikalische Chemie 19 (1932) 203–216, https://doi.org/10.1515/zpch-1932-0120.

[25] F. Louis, C.A. Gonzalez, R.E. Huie, M.J. Kurylo, An ab initio study of the kinetics of the reactions of halomethanes with the hydroxyl radical. 1. CH_2Br_2, J. Phys. Chem. 104 (2000) 2931–2938, https://doi.org/10.1021/jp991022e.

[26] J. Tomasi, B. Mennucci, R. Cammi, Quantum mechanical continuum solvation models, Chem. Rev. 105 (2005) 2999–3094, https://doi.org/10.1021/cr9904009.

[27] A.D. Becke, Density-functional thermochemistry. III. The role of exact exchange, J. Chem. Phys. 98 (1993) 5648–5652, https://doi.org/10.1063/1.464913.

[28] M.J. Frisch, G.W. Trucks, H.B. Schlegel, G.E. Scuseria, M.A. Robb, J.R. Cheeseman, G. Scalmani, V. Barone, G.A. Petersson, H. Nakatsuji, X. Li, M. Caricato, A.V. Marenich, J. Bloino, B.G. Janesko, R. Gomperts, B. Mennucci, H.P. Hratchian, J.V. Ortiz, A.F. Izmaylov, J.L. Sonnenberg, D. Williams-Young, F. Ding, F. Lipparini, F. Egidi, J. Goings, B. Peng, A. Petrone, T. Henderson, D. Ranasinghe, V.G. Zakrzewski, J. Gao, N. Rega, G. Zheng, W. Liang, M. Hada, M. Ehara, K. Toyota, R. Fukuda, J. Hasegawa, M. Ishida, T. Nakajima, Y. Honda, O. Kitao, H. Nakai, T. Vreven, K. Throssell, J.A. Montgomery Jr., J.E. Peralta, F. Ogliaro, M.J. Bearpark, J.J. Heyd, E.N. Brothers, K.N. Kudin, V.N. Staroverov, T.A. Keith, R. Kobayashi, J. Normand, K. Raghavachari, A.P. Rendell, J.C. Burant, S.S. Iyengar, J. Tomasi, M. Cossi, J.M. Millam, M. Klene, C. Adamo, R. Cammi, J.W. Ochterski, R.L. Martin, K. Morokuma, O. Farkas, J.B. Foresman, D.J. Fox, Gaussian 16, Revision A.03, Gaussian, Inc., Wallingford CT, 2016.

[29] R. Bauernschmitt, R. Ahlrichs, Treatment of electronic excitations within the adiabatic approximation of time dependent density functional theory, Chem. Phys. Lett. 256 (1996) 454–464, https://doi.org/10.1016/0009-2614(96)00440-X.

[30] R.G. Parr, W. Yang, Density Functional Theory of Atoms and Molecules, Oxford Univ. Press, Oxford, 1989.

[31] T. Lu, F. Chen, Atomic dipole moment corrected Hirshfeld population method, J. Theor. Comput. Chem. 11 (2012) 163–183, https://doi.org/10.1142/S0219633612500113.

[32] A.D. McLean, G.S. Chandler, Contracted Gaussian basis sets for molecular calculations. I. Second row atoms, $Z = 11-18$, J. Chem. Phys. 72 (1980) 5639–5648, https://doi.org/10.1063/1.438980.

[33] R. Krishnan, J.S. Binkley, R. Seeger, J.A. Pople, Self-consistent molecular orbital methods. XX. A basis set for correlated wave functions, J. Chem. Phys. 72 (1980) 650–654, https://doi.org/10.1063/1.438955.

[34] T. Lu, F. Chen, Multiwfn: a multifunctional wavefunction analyzer, J. Comput. Chem. 33 (2012) 580–592, https://doi.org/10.1002/jcc.22885.

[35] S. Grimme, Semiempirical GGA-type density functional constructed with a long-range dispersion correction, J. Comput. Chem. 27 (2006) 1787–1799, https://doi.org/10.1002/jcc.20495.

[36] T. Schwabe, S. Grimme, Double-hybrid density functionals with long-range dispersion corrections: higher accuracy and extended applicability, Phys. Chem. Chem. Phys. 9 (2007) 3397–3406, https://doi.org/10.1039/B704725H.

[37] Y. Niu, Q. Peng, C. Deng, X. Gao, Z.G. Shuai, Theory of excited state decays and optical spectra: application to polyatomic molecules, J. Phys. Chem. 114 (2010) 7817–7831, https://doi.org/10.1021/jp101568f.

[38] Q. Peng, Y. Yi, Z.G. Shuai, J. Shao, Toward quantitative prediction of molecular fluorescence quantum efficiency: role of Duschinsky rotation, J. Am. Chem. Soc. 129 (2007) 9333–9339, https://doi.org/10.1021/ja067946e.

[39] E. Magid, B.O. Turbeck, The rates of the spontaneous hydration of CO_2 and the reciprocal reaction in neutral aqueous solutions between 0 ℃ and 38 ℃, BBA-Gen, Subjects 165 (1968) 515–524, https://doi.org/10.1016/0304-4165(68)90232-8.

[40] F.J. Millero, D. Pierrot, K. Lee, R. Wanninkhof, R. Feely, C.L. Sabine, R.M. Key, T. Takahashi, Dissociation constants for carbonic acid determined from field measurements. Deep sea research part I: oceanographic research papers deep-sea res. Part I-Oceanogr, Res. Pap. 49 (2002) 1705–1723, https://doi.org/10.1016/S0967-0637(02)00093-6.